THE ASTROPHYSICAL JOURNAL, 464:715–723, 1996 June 20


# EVIDENCE FOR ACCELERATION AND NONRADIAL MOTION OF PARSEC-SCALE JET COMPONENTS IN THE LOBE-DOMINATED SUPERLUMINAL QUASAR 3C 263

D. H. HOUGH,[1,2] J. A. ZENSUS,[3] AND R. W. PORCAS[4]

*Received 1995 September 5; accepted 1996 January 8*

## ABSTRACT

We report evidence for accelerated and nonradial motion of parsec-scale jet components in the nucleus of the lobe-dominated quasar 3C 263. New VLBI maps at 10.7 GHz confirm that the jet component J1 moves with superluminal speed. While the initial apparent transverse velocity of J1 was $v_{app} \sim 1.2\ h^{-1}\ c$ ($H_0 = 100\ h$ km s$^{-1}$ Mpc$^{-1}$, $q_0 = 0.5$), the new maps indicate an *average* $v_{app} \sim 2.2\ h^{-1}\ c$ over a span of $\sim 8$ yr. This suggests the possibility of component acceleration, which could most simply be accounted for in a relativistic jet model that allows time variations in the Lorentz factor. The new maps also reveal a second jet component J2 that has moved along a significantly different radial direction than J1 with respect to the core component C. Component J2 shows a marginal change in direction that may be bringing it into alignment with the path of J1. We estimate $v_{app} \sim 0.7\ h^{-1}\ c$ for J2. We also present a new 8.4 GHz VLBI map that will enable us to continue monitoring 3C 263 with the VLBA. We relate our results to other properties of 3C 263 and discuss their implications for relativistic jet models and "unified schemes." We conclude that the low superluminal speeds in many lobe-dominated quasars, together with the suggested mildly accelerated and nonradial motion exhibited by 3C 263, are consistent with unification of core- and lobe-dominated quasars.

*Subject headings:* galaxies: jets — galaxies: nuclei — quasars: individual (3C 263) — radio continuum: galaxies

## 1. INTRODUCTION

Quasars and active galactic nuclei exhibit substantial evidence for relativistic outflows, of which a detailed understanding is necessary to build physical models of individual sources and to devise "unified schemes" of active extragalactic objects (e.g., Pearson & Zensus 1987; Pearson 1990). Simple relativistic beaming models have been proposed to describe these outflows, most often characterized as "jets." Such models often assume a narrow emission cone and a single Lorentz factor $\gamma$ for the jet, and attempt to account for the diversity of active extragalactic objects largely in terms of jet orientation effects (e.g., Scheuer & Readhead 1979; Blandford & Königl 1979; Orr & Browne 1982; Barthel 1989). While such models are oversimplified, it is nonetheless critical to conduct rigorous observational tests of them to ascertain what modifications may be necessary to achieve a better understanding of radio source physics.

As a direct challenge to early versions of beaming models, Porcas (1981) made VLBI observations that revealed apparent superluminal motion in the "double-lobed," or "lobe-dominated," quasar 3C 179. A few "core-dominated" radio sources had previously been observed to show superluminal speeds up to $\sim 10\ h^{-1}\ c$ ($H_0 = 100\ h$ km s$^{-1}$ Mpc$^{-1}$, $q_0 = 0.5$ in the Friedmann cosmology we will assume throughout this paper). In fact, this coupling of strong cores with highly superluminal speeds provided much of the impetus for early versions of beaming models; a jet axis oriented near the line of sight afforded a straightforward explanation of these observations. A clear prediction of such models is that counterparts of the core-dominated sources oriented at large angles to the line of sight should tend to display mildly superluminal speeds of $\leq 2c$–$3c$ (e.g., Scheuer 1987). Since 3C 179 was selected on the basis of its dominant, presumably unbeamed lobe emission—thus making it likely that its jet axis points at a relatively large angle to the line of sight—its moderately high superluminal speed (now estimated at $4.8\ h^{-1}c$; Porcas 1987) has proved somewhat problematic for beaming models.

This surprising result for 3C 179 was in part the motivation to begin two long-term VLBI surveys to determine the distribution of parsec-scale jet velocities in complete samples of lobe-dominated quasars with minimal orientation bias: one selected from the revised 3CR 178 MHz survey (Hough & Readhead 1989, hereafter HR89) and the other from the Jodrell Bank 966 MHz survey (Zensus & Porcas 1987, hereafter ZP87). (For our purposes, a lobe-dominated quasar is defined as having a ratio $R$ of nuclear to extended flux density at an emitted frequency of 5 GHz less than $\sim 1$.) These samples are particularly well suited for statistical tests of radio source models, whether or not their optical identification as quasars reintroduces any orientation bias as in some quasar-radio galaxy unification schemes (e.g., Owen 1986; Scheuer 1987; Barthel 1989), as long as the bias can be quantified. *In fact, our VLBI surveys offer the opportunity to test not only unified beaming models in quasars but also the more general question of quasar–radio galaxy unification.*

The primary objective in each survey must be to obtain a measure of the parsec-scale jet speed for every source in the sample as rapidly as possible (there are approximately 50 sources in the combined samples). To date, we have reported superluminal velocities $v_{app}$ or upper limits for eight objects in our two samples (ZP87; Hough, Vermeulen, & Readhead 1993; Hough et al. 1993). The results have been intriguing: the observed range of $v_{app} \sim 1$–$5\ h^{-1}c$ is consistent with simple beaming models, and we expect the pace of

[1] Department of Physics, Trinity University, San Antonio, TX 78212.
[2] Jet Propulsion Laboratory, California Institute of Technology, Pasadena, CA 91109.
[3] National Radio Astronomy Observatory, Edgemont Road, Charlottesville, VA 22903.
[4] Max-Planck-Institut für Radioastronomie, Auf dem Hügel 69, D-53121 Bonn, Germany.

TABLE 1

JOURNAL OF OBSERVATIONS

| Epoch | Stations[a,b] | Frequency (GHz) | Bandwidth (MHz) | Duration of Observations (hr) | CLEAN Beam[c] (mas,°) |
|---|---|---|---|---|---|
| 1981.76..... | BKGFO | 10.7 | 56 | 6 | ... |
| 1982.75..... | BKG(F)O | 10.7 | 56 | 12 | 0.52 × 0.48, 90 |
| 1983.78..... | BK(GF)O | 10.7 | 28/56 | 14 | 0.51 × 0.42, −20 |
| 1984.94..... | BLKGO | 10.7 | 28 | 12 | 0.48 × 0.46, −45 |
| 1989.27..... | BKGPO | 10.7 | 28 | 14 | 0.50 × 0.48, 57 |
| 1991.15..... | BLKGPO | 10.7 | 28 | 9 | 0.51 × 0.40, −39 |
| 1991.17..... | BLTKGYPCO | 8.4 | 28 | 9 | 0.73 × 0.44, −39 |

[a] Station legend: B = Max-Planck-Institut für Radioastronomie, Effelsberg, Germany (100 m telescope); L = Istituto di Radioastronomia, Medicina, Italy (32 m telescope); T = Onsala Space Observatory, Onsala, Sweden (20 m telescope); K = Haystack Observatory, Westford, MA (37 m telescope); G = National Radio Astronomy Observatory (NRAO), Green Bank, WV (43 m telescope); F = George R. Agassiz Station, Fort Davis, TX (26 m telescope); Y = NRAO Very Large Array, Socorro, NM (27 × 25 m telescope); P = NRAO Very Long Baseline Array (VLBA), Pie Town, NM (25 m telescope); C = NRAO VLBA, Kitt Peak, AZ (25 m telescope); O = Owens Valley Radio Observatory, Big Pine, CA (40 m telescope).

[b] Fringes were found to stations in parentheses, but the data were not used in our final analysis.

[c] CLEAN beam parameters are the FWHM of the major and minor axes of the elliptical Gaussian restoring beam and the P.A. of the major axis.

our surveys to increase dramatically with the Very Long Baseline Array (VLBA) (Napier et al. 1994). In these studies, however, a small number of objects have emerged as being particularly amenable to multiple-epoch observations. These objects allow us to perform observations akin to the monitoring done on the well-known core-dominated superluminal sources: they provide valuable case studies of the time evolution of structure in the nuclei of lobe-dominated superluminal objects.

One such object is the lobe-dominated quasar 3C 263 = 1137+660, which is optically identified as a variable quasar with visual magnitude $m_V = 16$ and redshift $z = 0.652$ (Hewitt & Burbidge 1993), and has a moderately strong radio nucleus with $R = 0.10$ (e.g., $R$ ranges from $\sim$0.001 to $\sim$1 in the sample of HR89). Superluminal motion with $v_{app} = 1.3\ h^{-1}c$ in the nucleus of 3C 263 was reported by Zensus, Hough, & Porcas (1987, hereafter ZHP87) based on three 10.7 GHz observing epochs in 1982, 1983, and 1984. In this paper, we present VLBI observations of 3C 263 at two further 10.7 GHz epochs (in 1989 and 1991), and at a single 8.4 GHz epoch (also in 1991) that is intended to provide continuity for monitoring 3C 263 at this standard VLBA frequency in the future. We report continued superluminal motion in 3C 263, with evidence for both accelerated and nonradial motion. Some possible explanations of these motions are offered. We then relate our results to those for other known superluminal sources and discuss them in the context of relativistic beaming and unified source models.

## 2. OBSERVATIONS, PROCESSING, AND ANALYSIS

The nucleus of 3C 263 had earlier been observed with VLBI arrays at a frequency of 10.7 GHz at a total of four epochs. A total of five $\sim$13 minute scans, spread over a $\sim$6 hr interval, were made at epoch 1981.76 during a pilot survey to detect resolved structure in several quasars (Hough 1986). Three subsequent full ($u$, $v$) track mapping experiments were performed at epochs 1982.75, 1983.78, and 1984.94, and the results were presented in ZHP87. We have now made 10.7 GHz mapping observations at two additional epochs, 1989.27 and 1991.15, and we have also made 8.4 GHz mapping observations at epoch 1991.17. The total observing interval for the mapping observations was on average $\sim$12 hr. The VLBI arrays included telescopes of the European VLBI network, the US VLBI network, and the National Radio Astronomy Observatory.[5] The data were recorded with the wideband Mark III system (Rogers et al. 1983). A journal of the observations for all seven epochs is given in Table 1.

The data were correlated on the Mark III/IIIA processors at Haystack Observatory and the Max-Planck-Institut für Radioastronomie, where fringe-fitting for each scan ($\leq$13 minutes) and coherent averaging to shorter intervals (1–6.5 minutes) were also performed.

All analysis was performed using the Caltech VLBI software package (Pearson 1991). The data were edited and calibrated in standard fashion. All 10.7 GHz maps presented here were made with the AMPHI, INVERT, and CLEAN routines. Confirmation of structures on these maps was made, in many cases using the DIFMAP imaging software (Shepherd, Pearson, & Taylor 1994) and the VLBMEM routine based on the maximum entropy method (MEM) (Gull & Daniell 1978). With the large number of stations at 8.4 GHz, however, we found that DIFMAP provides both a considerably better fit to the data and a clearly superior dynamic range (by a factor of $\sim$3) than the AMPHI, INVERT, and CLEAN routines. Therefore, here we present the 8.4 GHz map obtained with DIFMAP. Models consisting of Gaussian components were fitted to the data with MODELFIT, and uncertainties in model parameters were estimated using ERRFIT and by visual inspection of fits to the data. The model parameters from MODELFIT are generally quite consistent with the maps.

## 3. RESULTS

### 3.1. *Structure*

The apparent structure of the nucleus in 3C 263 can be well represented by two or three Gaussian components at

[5] The National Radio Astronomy Observatory is operated by Associated Universities, Inc., under cooperative agreement with the National Science Foundation.

TABLE 2

MODEL-FITTING RESULTS[a]

| Epoch | $S_{max}$[b] (mJy) | Component | $S$[c] (mJy) | $r$[d] (mas) | P.A.[d] (deg) | $D$[e] (mas) |
|---|---|---|---|---|---|---|
| 1981.76..... | ~150 | C | 80 ± 20 | 0 | 0 | 0[f] |
| | | J1 | 30 ± 20 | 0.6 ± 0.3 | 117 ± 13 | 0[f] |
| 1982.75..... | ~170 | C | 95 ± 15 | 0 | 0 | 0.1 ± 0.1 |
| | | J1 | 74 ± 20 | 0.48 ± 0.02 | 110 ± 2 | 0.2 ± 0.1 |
| 1983.78..... | ~150 | C | 86 ± 10 | 0 | 0 | 0.1 ± 0.1 |
| | | J1 | 45 ± 10 | 0.53 ± 0.02 | 108 ± 2 | 0.1 ± 0.1 |
| 1984.94..... | ~160 | C | 103 ± 10 | 0 | 0 | <0.1 |
| | | J1 | 52 ± 10 | 0.61 ± 0.03 | 109 ± 2 | 0.5 ± 0.1[g] |
| 1989.27..... | ~140 | C | 77 ± 4 | 0 | 0 | 0.07 ± 0.06 |
| | | J2 | 29 ± 3 | 0.37 ± 0.03 | 116 ± 2 | <0.22 |
| | | J1 | 24 ± 7 | 1.15 ± 0.03 | 110 ± 2 | 0.34 ± 0.12 |
| | | J0? | 4 ± 4 | 2.4 ± 0.3 | 113 ± 5 | 0.3 ± 0.3 |
| 1991.15..... | ~130 | C | 74 ± 6 | 0 | 0 | 0.1 ± 0.1 |
| | | J2 | 23 ± 6 | 0.42 ± 0.04 | 111 ± 3 | 0.1 ± 0.1 |
| | | J1 | 24 ± 10 | 1.24 ± 0.10 | 110 ± 3 | 0.4 ± 0.1 |
| 1991.17..... | ~110[h] | C | 60 ± 4 | 0 | 0 | <0.15 |
| | | J2 | 21 ± 3 | 0.56 ± 0.06 | 113 ± 4 | 0.19 ± 0.16 |
| | | J1 | 18 ± 4 | 1.28 ± 0.08 | 111 ± 2 | 0.25 ± 0.19 |
| | | J0 | 7 ± 3 | 2.4 ± 0.2 | 113 ± 2 | 0.4 ± 0.4 |

[a] Uncertainties in the component parameters were determined by visual inspection and by use of G. Comoretto's ERRFIT routine in the Caltech VLBI software package.

[b] $S_{max}$ is the maximum correlated flux density on short baselines (~[15–30] × $10^6$ wavelengths).

[c] $S$ is the flux density.

[d] $r$ and P.A. give the separation and position angle, respectively, of the component relative to the assumed core C.

[e] $D$ is the FWHM diameter of a circular Gaussian component; upper limits are given in cases where point components give the best fits.

[f] At epoch 1981.76, two point components were assumed.

[g] At epoch 1984.94, component J1 is elliptical, with an axial ratio of 0.3 ± 0.3 and P.A. = 103° ± 20°.

[h] At epoch 1991.17, even the very short YP baseline (~1 × $10^6$ wavelengths) also has $S_{max}$ ~ 110 mJy.

each epoch, as given in Table 2. At epoch 1981.76, we had insufficient data to constrain the component shapes or sizes and simply fitted two point components. There are two components that we label C and J1 (note that these were referred to as W and E, respectively, in ZHP87) at a separation <1 milliarcsecond (mas). Barthel et al. (1984) also found evidence for milliarcsecond-scale structure at the lower frequency of 5 GHz at epoch 1981.3, based on correlated flux densities ranging from ~100 to ~200 mJy. At epochs 1982.75, 1983.78, and 1984.94, we fitted two Gaussian components for C and J1. In the more recent observations at epochs 1989.27, 1991.15, and 1991.17, however, a new component has emerged from the core that we label J2; thus we fitted three Gaussian components to the main structure for these last three epochs. CLEAN maps at conventional resolution are shown for all five 10.7 GHz mapping epochs in Figure 1, and for the 8.4 GHz mapping epoch in Figure 2. We note that there is generally good agreement of the component positions on the nearly simultaneous epoch 1991.15 10.7 GHz and epoch 1991.17 8.4 GHz maps, although there is a significant discrepancy (~0.1 mas) in the separation between C and J2. This discrepancy could be due to, e.g., opacity effects in the source or calibration errors; but whatever its cause, it demonstrates the value of obtaining nearly simultaneous 8.4 and 10.7 GHz maps to permit a smooth transition to the new monitoring frequency of 8.4 GHz with the VLBA. There is essentially no evidence for emission beyond ~3 mas in the maps, and the models basically all contain a flux density equal to the maximum correlated flux density on the short baselines. Barthel et al. (1985) presented a model at 5 GHz at epoch 1982.3, containing 200 mJy in a single elliptical Gaussian component, with a FWHM of 0.8 × 0.5 mas, and oriented along a position angle (P.A.) of 110°. They stated that there was evidence for structure on larger scales, but it is not clear if this would have extended beyond ~3 mas.

Inspection of the models in Table 2 shows modest but clear variations in the flux density of component C, which is usually the most compact and which we identify as the core. Component C dropped from an average of ~95 mJy for epochs 1982.75–1984.94 to ~75 mJy at epochs 1989.27 and 1991.15. The components J1 and J2 are identified as jet features. For the older component J1, the flux density dropped by a factor of ~3 between epochs 1982.75 and 1991.15. This decrease occurred in stages, with a drop from ~75 mJy at epoch 1982.75 to ~50 mJy at epochs 1983.78 and 1984.94, and then a further drop to ~25 mJy at epochs 1989.27 and 1991.15. This component was extended at epoch 1984.94 and appeared so again at the later epochs; there is no clear indication that the component size has changed over time. The newer jet component J2 is very compact, and it had an average flux density of ~25 mJy at epochs 1989.27 and 1991.15, essentially compensating for the decrease experienced by C. Note that J2 is similar in strength to J1 at both of these later epochs, but J2 is therefore 3 times weaker than J1 was when observed at a similar distance (~0.4–0.5 mas) from C.

Some of the mildly superresolved maps (see § 3.3), particularly at epoch 1991.15, show hints of a weak, curved bridge of emission that links J2 to J1. However, model-fitting results for C, J1, and J2 are not significantly altered by the inclusion of an extra component to represent this possible

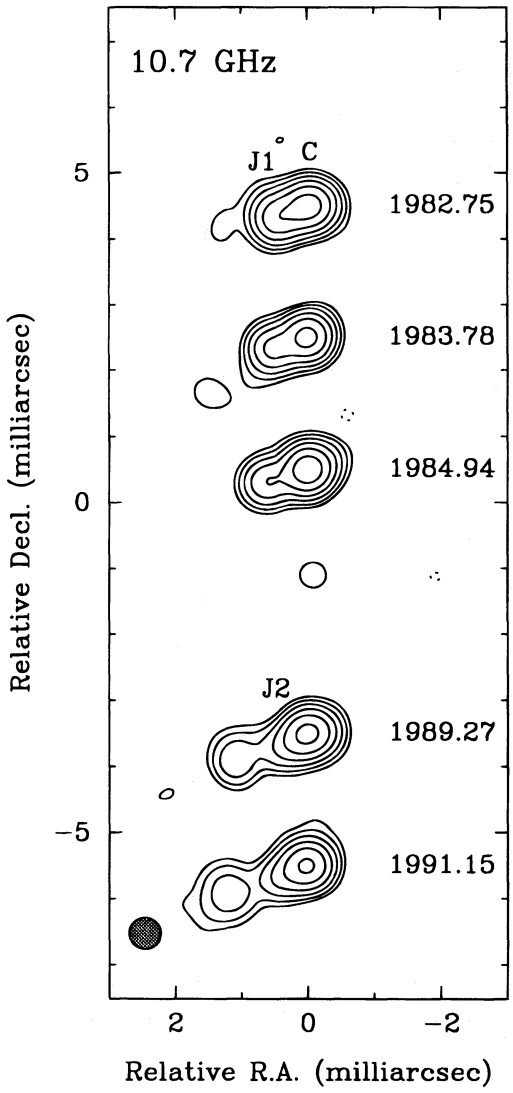


FIG. 1.—CLEAN maps of the nucleus of 3C 263, at the five 10.7 GHz epochs 1982.75, 1983.78, 1984.94, 1989.27, and 1991.15. Components C, J1, and J2 are labeled where they first appear. The contours are −2 (*dotted*), 2, 4, 8, 16, 32, and 64 mJy beam$^{-1}$. CLEAN models have been convolved with a circular restoring beam of FWHM = 0.48 mas, which is shown shaded, and represents the average of the beam sizes in Table 1. CLEAN maps have been aligned assuming that component C is stationary.

bridge of emission, and we do not consider it further. Also, there is good evidence for the presence of an additional jet component beyond J1, ~2.4 mas from C on the 8.4 GHz map at epoch 1991.17; this component is marginally detected at a similar distance on the 10.7 GHz map at epoch 1989.27. We label this component J0, and we have included it in our model fitting at these two epochs. Unfortunately, there is no significant evidence for such a component at any other epochs.

### 3.2. *Motion of Component J1*

An internal proper motion $\mu = 0.06 \pm 0.02$ mas yr$^{-1}$ of J1 relative to C was reported for epochs 1982.75–1984.95 by ZHP87; the quoted uncertainty from model fitting is a conservative "limit of error" value based only on the two epochs 1982.75 and 1984.94. A straightforward weighted least-squares fit to the data for all three of the epochs 1982.75, 1983.78, and 1984.94 yields $\mu = 0.058 \pm 0.007$ mas yr$^{-1}$. The reduced $\chi^2$ value for the fit $\chi^2_\nu = 0.17$, with a corresponding probability $P = 0.68$ that discrepancies between the fit and the data occur by chance. Within the uncertainties, this motion occurred along a constant position angle, with an average P.A. = 109°. At epochs 1989.27 and 1991.15, J1 showed continued motion away from C along the same P.A. of 110° originally found on the map at epoch 1982.75. Based on the model-fitting results, we calculate $\mu = 0.048 \pm 0.056$ mas yr$^{-1}$ for J1 between these two later epochs, which is highly uncertain but consistent with the value found for the three earlier epochs.

However, if we plot the separation of C and J1 for all five 10.7 GHz mapping epochs versus time (Fig. 3), it is *not* entirely clear that the expansion rate has been constant. For example, the piecewise linear fits to the earlier and later epochs given above, which have similar values of $\mu$, do not match up in the interval between 1984.94 and 1989.27. While we do not have sufficient data to warrant a full exploration of complex scenarios for the motion of J1, a few simple cases are worthy of investigation.

In the absence of data for the crucial interval between 1984.94 and 1989.27, we entertain three possible cases for the motion of J1: (1) constant velocity; (2) an alternative piecewise linear form that would match the two fits by assuming a sudden, brief acceleration after 1984.94; and (3) uniform positive acceleration. We will adopt the criterion that a fit is acceptable if the $\chi^2$ test yields $P \geq 0.10$. In case 1, a linear fit yields $\mu = 0.103 \pm 0.009$ mas yr$^{-1}$, which is about *twice* the original proper motion. However, $\chi^2_\nu = 3.33$ and $P = 0.02$, which suggests that a simple linear fit does not represent the data very well. In case 2, a fit to epochs 1984.94–1991.15 gives $\mu = 0.12 \pm 0.01$ mas yr$^{-1}$, again about twice the original proper motion; the fit is acceptable, with $\chi^2_\nu = 1.74$ and $P = 0.19$. In case 3, a second-order polynomial fit has $\chi^2_\nu = 2.26$ and $P = 0.10$, which is marginally acceptable. The equation for the fit is $r = 0.3656 + 0.02025t + 0.006615t^2$, where $r$ is the component separation (in mas) and $t$ is the time elapsed since 1980.0 (in years). Thus, both cases that assume some form of accelerated motion for component J1 appear acceptable by our definition, while the case that assumes constant velocity does not. The linear fits for cases 1 and 2 are shown in Figure 3.

We note that it is unlikely that a systematic offset in the measurement of component separations at the earlier or later epochs could create an apparent departure from a true motion at constant velocity. From a comparison of the weighted least-squares fit line in Figure 3 for the epochs 1982.75–1984.94 with the actual data for epochs 1989.27 and 1991.15, it is clear that any such offset would have to approach ~0.3 mas, which is well over half the conventional synthesized beamwidth (~0.5 mas). The core component C appears very compact (best-fit FWHM diameter ≤0.1 mas at all epochs), which rules out shifting of the core's brightness centroid as the cause of such a large offset. It should be noted, however, that undetected random shifting of the core's position (e.g., by ±0.05 mas, less than its FWHM diameter) could produce apparent departures from actual motion at constant speed.

### 3.3. *Motion of Component J2*

The newer jet component, J2, was first observed at epoch 1989.27 and again at epoch 1991.15. This component

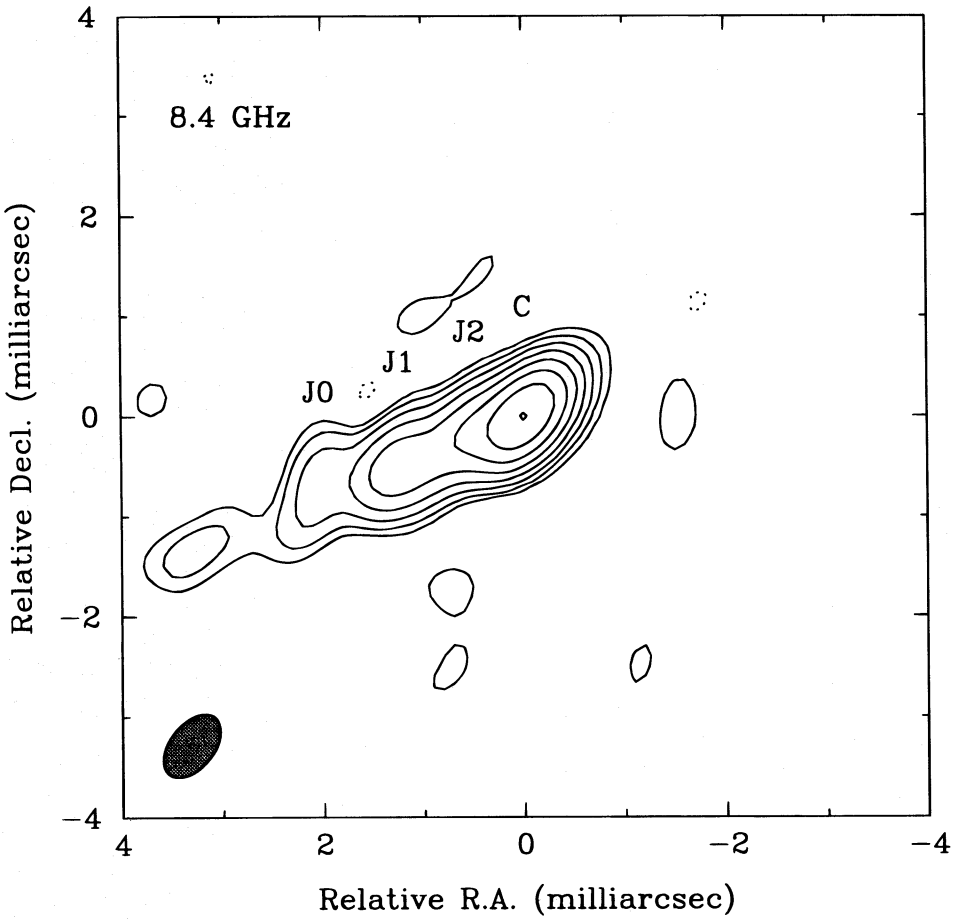


FIG. 2.—CLEAN map of the nucleus of 3C 263, at 8.4 GHz at epoch 1991.17. Components C, J0, J1, and J2 are labeled. Contours are −0.5 (*dotted*), 0.5, 1, 2, 4, 8, 16, 32, and 64 mJy beam$^{-1}$. The elliptical restoring beam with FWHM 0.73 × 0.44 mas in P.A. −39° is shown shaded.

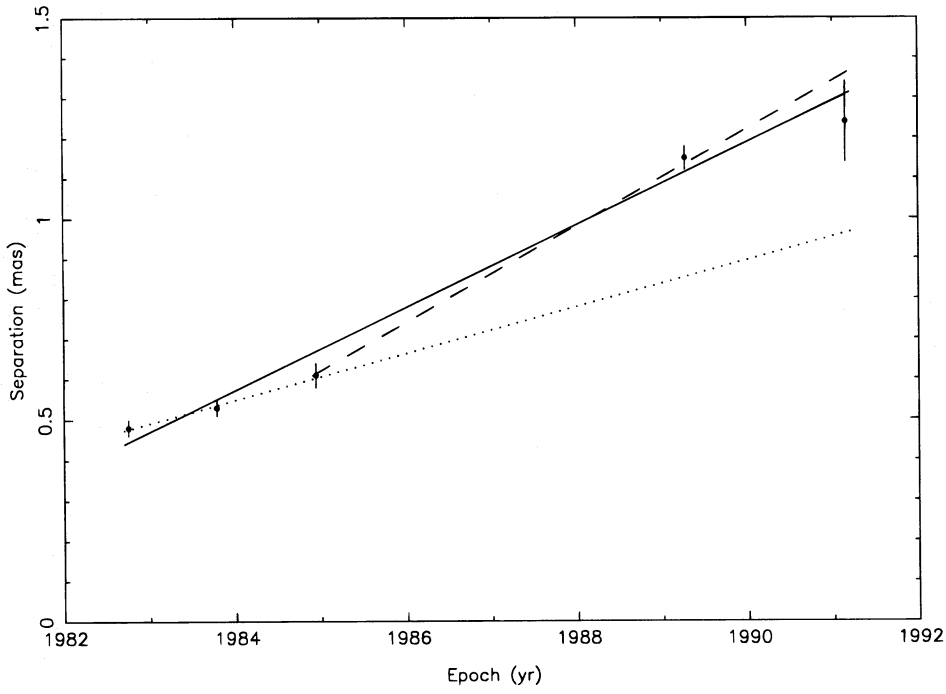


FIG. 3.—Separation of components C and J1 (mas) in 3C 263 vs. observing epoch (yr), at the five 10.7 GHz mapping epochs. *Dotted line:* a weighted least-squares fit for epochs 1982.75 through 1984.94, with an extrapolation to epoch 1991.15 shown; it represents a constant proper motion $\mu = 0.058 \pm 0.007$ mas yr$^{-1}$. *Dashed line:* a weighted least-squares fit for epochs 1984.94 through 1991.15; it represents a constant proper motion $\mu = 0.12 \pm 0.01$ mas yr$^{-1}$. *Solid line:* a weighted least-squares fit for epochs 1982.75 through 1991.15; it represents a constant proper motion $\mu = 0.103 \pm 0.009$ mas yr$^{-1}$.

appears as an extension to the southeast of the core on the CLEAN maps in Figure 1. Superresolved CLEAN maps for epochs 1989.27 and 1991.15 are displayed in Figure 4. It is clear that J2 was at a larger P.A. ($\sim 115°$) than the older jet component J1 at epoch 1989.27. MEM and superresolved CLEAN maps suggest that the contours of J2 extend along a P.A. as large as $\sim 120°$, while model fitting yields P.A. $\sim 116°$. By epoch 1991.15, J2 appeared to be at P.A. $\sim 113°$ on the maps and $\sim 111°$ from the model fitting.

At epoch 1991.15, J2 appeared to become slightly more distinct from the core component C, mildly suggesting outward motion. At epoch 1989.27, the maps do not yield reliable estimates of the separation between C and J2, but model-fitting yields a separation of $0.37 \pm 0.03$ mas. At epoch 1991.15, model fitting yields $0.42 \pm 0.04$ mas, in agreement with the maps. Taking into account the change in position angle as well, we calculate the *total* internal proper motion of J2 to be $\mu = 0.032 \pm 0.024$ mas yr$^{-1}$.

## 4. DISCUSSION

### 4.1. *Structure*

We interpret the milliarcsecond-scale structure in the nucleus of 3C 263 as a standard "core-jet." Component C is assumed to be the core on the basis of its compactness at all epochs. The components J1 and J2 are identified as knots in the jet; the extended size of J1 in particular lends support to this interpretation. The jet components lie on the same side of the core as the one-sided arcsecond-scale jet imaged with the VLA at 5 GHz by Bridle et al. (1994). In fact, the average P.A. for the jet knot J1 at the five 10.7 GHz mapping epochs is 109°, which matches exactly the P.A. of the straight, essentially continuous, $\sim 12''$ inner segment of the arcsecond-scale jet. There are departures from this striking linearity, however, at the innermost and outermost parts of the jet. The component J2 first emerged at P.A. $\sim 116°$, within $\sim 0.4$ mas of component C, before appearing to begin to align with the straight segment of the jet just beyond this distance. The arcsecond-scale jet bends southward $\sim 15''$ from the nucleus, just prior to its termination at the hot spot in the eastern lobe. The hot spot lies $\sim 16''$ from the nucleus in P.A. = 112°. The largest angular size of 3C 263 is $51''$, corresponding to a linear size of $200\ h^{-1}$ kpc.

### 4.2. *Variability*

The nucleus of 3C 263 was classified by HR89 as variable with amplitude of variation greater than 40 mJy at 5 GHz. The record of 5 GHz nuclear flux densities obtained by interferometric observations with arcsecond-scale resolution is given in Table 3. Although these values range from 130 to 194 mJy, it is actually not clear if the variations are statistically significant, in part because no uncertainties were quoted in the references for the VLA snapshot observ-

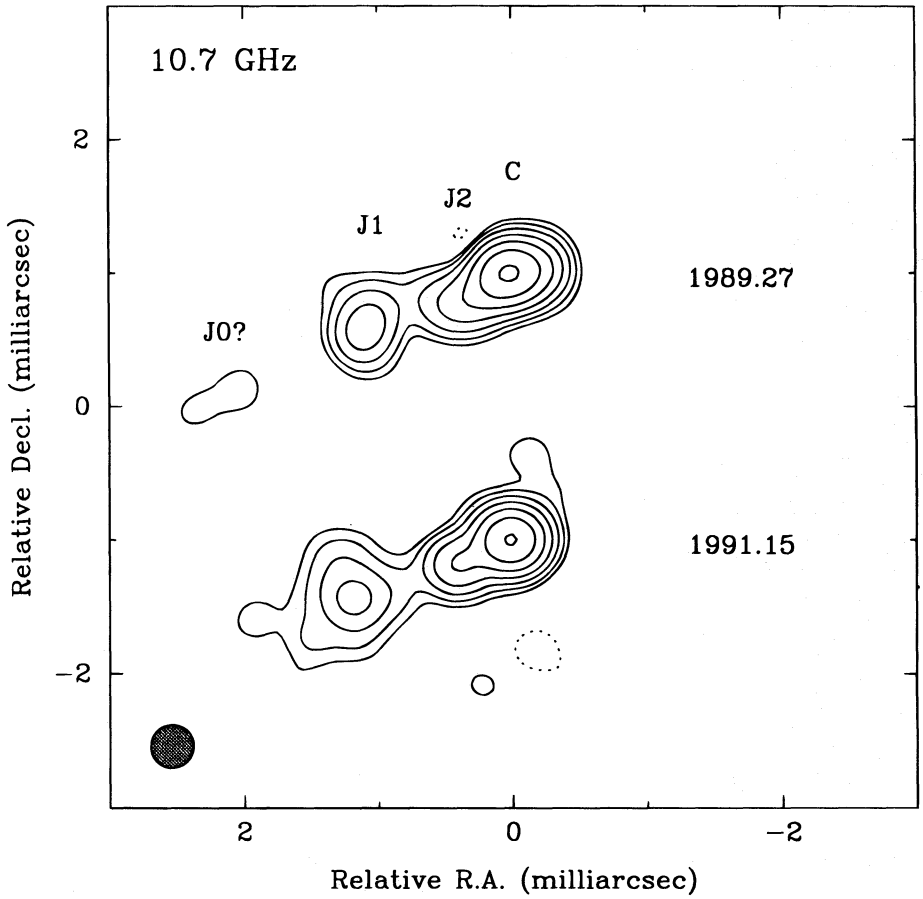


FIG. 4.—Superresolved CLEAN maps of the nucleus of 3C 263, at the two 10.7 GHz epochs 1989.27 and 1991.15. Components C, J1, and J2 are labeled, as is the marginally detected weak component J0. The contours are −1 (*dotted*), 1, 2, 4, 8, 16, 32, and 64 mJy beam$^{-1}$. CLEAN models have been convolved with a circular restoring beam of FWHM = 0.32 mas, which is shown shaded, and represents two-thirds of the average conventional beam size used in Fig. 1.

TABLE 3

5 GHz Flux Density History of the Nucleus of 3C 263

| Epoch | Flux Density[a] (mJy) | Synthesis Telescope | Reference |
|---|---|---|---|
| ~1973..... | 130 ± 20 | Cambridge 5 km | Pooley & Henbest 1974 |
| 1973.8 ± 0.5..... | 162 ± 8 | Westerbork | Miley & Hartsuijker 1978 |
| 1979.5 ..... | 194 | VLA (snapshot) | Schilizzi, Kapahi, & Neff 1982 |
| 1981.2 ..... | 169 | VLA (snapshot | Swarup, Sinha, & Hilldrup 1984 |
| 1983.7 ..... | 146 | VLA (snapshot) | Reid et al. 1995 |
| 1987.7 ..... | 157 ± 0.5 | VLA (full synthesis) | Bridle et al. 1994 |

[a] No uncertainty quoted by references for VLA snapshots.

ations. The plausible assumption of a 5% uncertainly fails to yield an acceptable linear fit (slope $-0.7 \pm 0.9$ mJy yr$^{-1}$, $\chi_\nu^2 = 4.59$, $P = 0.001$), so for the discussion below we will assume that the variations are statistically significant.

It would be useful to relate the appearance of VLBI jet components to flux density outbursts. This has been done for the lobe-dominated quasar 3C 245 (Hough & Readhead 1987; Hough et al. 1996) and, of course, for many of the core-dominated quasars (e.g., Zensus, Krichbaum, & Lobanov 1995). Although there is no sharply defined outburst in 3C 263, the data are consistent with a monotonic rise in flux density from ~130 mJy around 1973 to ~190 mJy at epoch 1979.5. If we make the simplifying assumption of a constant proper motion $\mu = 0.058 \pm 0.007$ mas yr$^{-1}$ prior to epoch 1984.94, the extrapolated time of origin of component J1 at the core C is 1974.5 ± 0.8. Thus, it may be possible to associate the appearance of J1 with the observed increase by ~60 mJy from 1973 to 1979. The large uncertainty in $\mu$ for component J2 does not warrant attempts to associate its appearance with a flux density event.

### 4.3. *Spectra of the VLBI Components*

Our nearly simultaneous epoch 1991.15 10.7 GHz and epoch 1991.17 8.4 GHz maps permit a determination of the spectral index $\alpha$ ($S \propto \nu^\alpha$) for each of the VLBI components C, J1, and J2 between these two frequencies, albeit with large uncertainties. We find $\alpha = 0.9 \pm 0.5$ for component C, $1.2 \pm 1.6$ for J1, and $0.4 \pm 1.1$ for J2. Thus, there is a weak suggestion of an inverted spectrum for the jet component J1, and a stronger suggestion thereof for the core C. We expect to find inverted spectra for the dominant milliarcsecond-scale components, since flux density measurements for the arcsecond-scale nucleus between 408 MHz and 15 GHz suggest an overall inverted spectrum with $\alpha \sim 0.3$ (Owen, Porcas, & Neff 1978; Reid et al. 1995; Wardle 1995). The spectra of the VLBI components in 3C 263 stand in contrast to those in the lobe-dominated quasar 4C 34.37 (Hooimeyer et al. 1992), which has a flat-spectrum ($\alpha \sim 0$) core and a steep-spectrum ($\alpha \sim -0.5$ to $-0.9$) jet. We note that milliarcsecond-scale jets with spectra steeper than the cores are observed in core-dominated quasars (e.g., Zensus, Cohen, & Unwin 1995).

### 4.4. *Accelerated Superluminal Motion of Jet Component J1*

The internal proper motion $\mu = 0.058 \pm 0.007$ mas yr$^{-1}$ of the older jet component J1 between epochs 1982.75 and 1984.94 corresponds to an apparent transverse velocity $v_{\rm app} = (1.2 \pm 0.1)\ h^{-1}\ c$. We find $\mu = 0.048 \pm 0.056$ mas yr$^{-1}$ between epochs 1989.27 and 1991.15, which yields $v_{\rm app} = (1.0 \pm 1.2)\ h^{-1}\ c$. These results are consistent with J1 having the same, barely superluminal speed at both the earlier three and the later two epochs.

However, a constant velocity only slightly greater than $h^{-1}\ c$ is not permitted by the plot of the separation between components C and J1 for epochs 1982.75 through 1991.15 (see Fig. 3). The proper motion in our case 1—a simple linear fit over this full time span—is $\mu = 0.103 \pm 0.009$ mas yr$^{-1}$, which corresponds to $v_{\rm app} = (2.2 \pm 0.2)\ h^{-1}\ c$. However, this simple linear fit is poor as judged by the $\chi^2$ test. In our case 2—the piecewise linear fits that match at epoch 1984.94—the fit after 1984.94 gives $\mu = 0.12 \pm 0.01$ mas yr$^{-1}$, which corresponds to $v_{\rm app} = (2.5 \pm 0.2)\ h^{-1}\ c$. Once again, judging by the $\chi^2$ test, each of the piecewise linear fits in case 2 is good, and the uniform acceleration curve in case 3 is satisfactory. *We therefore conclude that there is some evidence, although not overwhelming, for accelerated motion of the jet component J1.* For comparison, we note that Hooimeyer et al. (1992), while not arguing for acceleration, did report two components at different distances from the core moving with different superluminal speeds in the lobe-dominated quasar 4C 34.47. Following Zensus et al. (1995), we will now consider two alternatives to explain the possibly accelerated motion of component J1: (1) changes in the angle of the jet axis to the line of sight, $\theta$, at constant Lorentz factor, $\gamma$; and (2) changes in $\gamma$ at constant $\theta$.

For the first alternative, we will assume a constant-$\gamma$ beaming model and $h = 1$. The larger of the two speeds from the matched piecewise linear fits, $v_{\rm app} = 2.5c$, then requires a minimum Lorentz factor $\gamma_{\rm min} = 2.7$ and an associated angle of the jet axis to the line of sight $\theta(\gamma_{\rm min}) = 22°$. We will set $\gamma = \gamma_{\rm min} = 2.7$. If J1 accelerates from $v_{\rm app} = 1.2c$ to $2.5c$ as the jet bends *away* from the line of sight, then $\theta$ must increase from 6° to 22°. However, a bend even as large as ~5° appears contrived, given the constancy of the P.A. of J1 to within 1° in the plane of the sky. The assumption of a larger, but still constant, value of $\gamma$ does not help to alleviate these difficulties; even for $\gamma = 10$, bends of ~35° are required.

For the second alternative, we will assume a constant-$\theta$ beaming model and $h = 1$. If we adopt $\gamma = \gamma_{\rm min} = 2.7$ and $\theta = \theta(\gamma_{\rm min}) = 22°$ for the larger speed $v_{\rm app} = 2.5c$ as above, then the lower speed $v_{\rm app} = 1.2c$ in the matched piecewise linear fits requires $\gamma = 1.7$ for $\theta = 22°$. Although this means that $\gamma$ needs to change by less than a factor of ~2, a possible difficulty with $\theta = 22°$ is that the deprojected linear size of 3C 263 is then 534 kpc, which is more than twice the largest projected linear size among the 3CR lobe-dominated quasars (247 kpc for 3C 47; HR89). This may not be problematic if quasar–radio galaxy unification holds and quasars are thus restricted to point within some maximum

value of $\theta$. However, since the quasar population may well be randomly oriented, it is worth considering alternative values of $\theta$. For example, $\gamma = 5$ and $\theta = 41°$ can account for the $v_{app} = 2.5c$ motion, which helps greatly to relieve the linear size problem. For $\theta = 41°$, we must then have $\gamma = 1.6$ for the $v_{app} = 1.2c$ motion. Thus, the linear size problem is much reduced at the expense of requiring slightly over a factor of $\sim 3$ change in $\gamma$.

We are thus led to conclude that of the two options considered, the case of constant $\theta$ and variable $\gamma$ appears to be favored for component J1. The physical cause of variations in $\gamma$ is not clear (e.g., Zensus et al. 1988; Vermeulen & Cohen 1994). Our conclusion is opposite to that reached by Zensus et al. (1995) for the core-dominated quasar 3C 345, in which—while not ruling out a constant-$\theta$ model—they favor a constant-$\gamma$ model to account for component accelerations. This seems plausible for 3C 345, where the required bending away from the line of sight is very modest ($\sim 3°$), even though the parsec-scale jet is observed to have bends approaching $\sim 70°$.

### 4.5. *Nonradial Motion of Jet Component J2*

Taken together, the models and maps suggest that component J2 experienced a *decrease* in P.A. of $\sim 5°$, from 115°–120° at epoch 1989.27 to 111°–113° at epoch 1991.15. The model-fitting results yield a formal decrease in P.A. of $5° \pm 4°$. While the evidence for nonradial motion of J2 is thus marginal, it is clear that J2 first appeared at a significantly *larger* P.A. ($116° \pm 2°$) than that of the path defined by J1 over five epochs ($109° \pm 1°$). *Therefore, we conclude that the jet components J1 and J2 have moved along significantly different radial directions with respect to the core component C, and that J2 exhibits marginal evidence of nonradial motion.* We note that component J1 was first observed $\sim 0.5$ mas from component C. If J2 experienced a real decrease in P.A. that brought it into alignment with J1 at $\sim 0.4$ mas from C, then this may indicate that collimation of the jet components along a 109° path occurs at $\sim 0.4$–$0.5$ mas, or $\sim 2$ pc projected distance, from the core.

The total proper motion for J2, $\mu = 0.032 \pm 0.024$ mas yr$^{-1}$, corresponds to $v_{app} = (0.7 \pm 0.5)\ h^{-1}\ c$. Thus, the motion of J2 is formally subluminal, although the large uncertainty does allow for a mildly superluminal speed. For $h = 1$, we find $\gamma_{min} = 1.2$ and $\theta(\gamma_{min}) = 55°$. The large uncertainty in $v_{app}$ does not warrant detailed attempts to model the motion of J2.

### 4.6. *Unified Schemes*

The apparent transverse velocities ranging from $\sim 0.7\ h^{-1}\ c$ to $\sim 2.5\ h^{-1}\ c$ in the nucleus of 3C 263 confirm the earlier conclusion of ZHP87 that the superluminal speed in this lobe-dominated quasar is substantially less than the speeds found in many well-studied core-dominated quasars. They also confirm the general tendency for superluminal speed to correlate with relative strength of the radio nucleus in the 3CR sample of lobe-dominated quasars (Vermeulen et al. 1993). These results are, to first order, consistent with simple relativistic beaming models and unification of core- and lobe-dominated quasars.

The evidence for mildly accelerated and nonradial motion reported here for 3C 263 strengthens the case for unification of core- and lobe-dominated quasars. These phenomena are predicted and observed to be more pronounced, e.g., in the case of the core-dominated quasar 3C 345, which is thought to have its jet oriented at very small angles to the line of sight ($\theta \sim 1°$–$4°$) (Zensus et al. 1995). The fact that the acceleration occurs at some distance removed from the core in both 3C 345 and 3C 263 further strengthens the connection between these two objects.

The acceleration in 3C 345 was successfully interpreted in terms of a constant-$\gamma$, variable-$\theta$ relativistic jet model (Zensus et al. 1995), in contrast to the constant-$\theta$, variable-$\gamma$ model favored here for component J1 in 3C 263. This raises the issue of whether a model allowing variations in both $\gamma$ and $\theta$ might generally be required to unify core- and lobe-dominated quasars.

It has been established that individual components follow different trajectories in 3C 345 (Zensus et al. 1995), but we have yet to observe jet components J1 and J2 over a similar range of distances from the core to determine whether this is true in 3C 263. Future monitoring with the VLBA will enable us to follow the motion of J2 and compare it with that of J1 beyond $\sim 0.5$ mas from the core.

## 5. CONCLUSIONS

We have confirmed superluminal motion in the nucleus of the lobe-dominated quasar 3C 263, and, in addition, we have discovered evidence for accelerated and nonradial motion of parsec-scale jet components. The range of apparent transverse velocities runs from somewhat subluminal ($\sim 0.7\ h^{-1}\ c$) for the inner jet component J2 to mildly superluminal ($\sim 1.2$–$2.5\ h^{-1}\ c$) for the outer jet component J1. The possible acceleration of component J1 is best understood in terms of a relativistic jet model that allows time variations in the Lorentz factor $\gamma$. Component J2 first appears at a distinctly different P.A. than J1, and shows marginal evidence of swinging into alignment with the path of J1. The relatively low superluminal speeds, together with the comparatively gentle acceleration and nonradial motion possibly occurring in 3C 263, all support unification of core- and lobe-dominated quasars. Statistical studies of the distribution of superluminal speeds in lobe-dominated quasars will now need to take into account accelerated motion. The completion of these studies (HR89; ZP87) is essential to test relativistic beaming models and unification scenarios.

We thank the staff at each observatory and at the Haystack and MPIfR processors for their valuable assistance. We thank L. L. Cross for her assistance with the reduction of the 8.4 GHz VLBI data. We are grateful to I. I. K. Pauliny-Toth for his careful reading of and comments on the manuscript. VLBI at the National Radio Astronomy Observatory, Haystack Observatory, George R. Agassiz Station, and the Owens Valley Radio Observatory received support from the National Science Foundation for these observations. Portions of this work were performed while D. H. H. held NRC-NASA Resident Research Associate and NASA-ASEE Summer Faculty Fellowship awards at the Jet Propulsion Laboratory, California Institute of Technology, under contract with the National Aeronautics and Space Administration. For other parts of this work, D. H. H. was supported by a Cottrell College Science Award of Research Corporation and NSF grant AST-9422075. J. A. Z. acknowledges support through the Humboldt Award of the Alexander-von-Humboldt Stiftung, to perform part of this research at the Max-Planck-Institut für Radioastronomie, Bonn.

## REFERENCES


Barthel, P. D. 1989, ApJ, 336, 606
Barthel, P. D., Miley, G. K., Schilizzi, R. T., & Preuss, E. 1984, A&A, 140, 399
———. 1985, A&A, 151, 131
Blandford, R. D., & Königl, A. 1979, ApJ, 232, 34
Bridle, A. H., Hough, D. H., Lonsdale, C. J., Burns, J. O., & Laing, R. A. 1994, AJ, 108, 766
Gull, S. F., & Daniell, G. J. 1978, Nature, 272, 686
Hewitt, A., & Burbidge, G. 1993, ApJS, 87, 451
Hooimeyer, J. R. A., Barthel, P. D., Schilizzi, R. T., & Miley, G. K. 1992, A&A, 261, 1
Hough, D. H. 1986, Ph.D. thesis, California Inst. Tech.
Hough, D. H., & Readhead, A. C. S. 1987, ApJ, 321, L11
———. 1989, AJ, 98, 1208 (HR89)
Hough, D. H., Vermeulen, R. C., & Readhead, A. C. S. 1993, in Sub-arcsecond Radio Astronomy, ed. R. J. Davis & R. S. Booth (Cambridge: Cambridge Univ. Press), 193
Hough, D. H., Vermeulen, R. C., Wood, Jr., D. A., Standifird, J. D., & Cross, L. L. 1996, ApJ, 459, 64
Hough, D. H., Zensus, J. A., Vermeulen, R. C., Readhead, A. C. S., Porcas, R. W., & Rius, A. 1993, in Sub-arcsecond Radio Astronomy, ed. R. J. Davis & R. S. Booth (Cambridge: Cambridge Univ. Press), 195
Miley, G. K., & Hartsuijker, A. P. 1978, A&AS, 34, 129
Napier, P. J., Bagri, D. S., Clark, B. G., Rogers, A. E. E., Romney, J. D., Thompson, A. R., & Walker, R. C. 1994, in Proc. IEEE, 82, 658
Orr, M. J. L., & Browne, I. W. A. 1982, MNRAS, 200, 1067
Owen, F. N. 1986, in IAU Symp. 119, Quasars, ed. G. Swarup, & V. K. Kapahi (Dordrecht: Reidel), 173
Owen, F. N., Porcas, R. W., & Neff, S. G. 1978, AJ, 83, 1009
Pearson, T. J. 1990, in Parsec-Scale Radio Jets, ed. J. A. Zensus & T. J. Pearson (Cambridge: Cambridge Univ. Press), 1
Pearson, T. J. 1991, BAAS, 23, 991
Pearson, T. J., & Zensus, J. A. 1987, in Superluminal Radio Sources, ed. J. A. Zensus & T. J. Pearson (Cambridge: Cambridge Univ. Press), 1
Pooley, G. G., & Henbest, S. N. 1974, MNRAS, 169, 477
Porcas, R. W. 1981, Nature, 294, 47
———. 1987, in Superluminal Radio Sources, ed. J. A. Zensus & T. J. Pearson (Cambridge: Cambridge Univ. Press), 12
Reid, A., Shone, D. L., Akujor, C. E., Browne, I. W. A., Murphy, D. W., Pedelty, J., Rudnick, L., & Walsh, D. 1995, A&AS, 110, 213
Rogers, A. E. E., et al. 1983, Science, 219, 51
Scheuer, P. A. G. 1987, in Superluminal Radio Sources, ed. J. A. Zensus & T. J. Pearson (Cambridge: Cambridge Univ. Press), 104
Scheuer, P. A. G., & Readhead, A. C. S. 1979, Nature, 277, 182
Schilizzi, R. T., Kapahi, V. K., & Neff, S. G. 1982, J. Astrophys. Astron., 3, 173
Shepherd, M. C., Pearson, T. J., & Taylor, G. B. 1994, BAAS, 26, 987
Swarup, G., Sinha, R. P., & Hilldrup, K. 1984, MNRAS, 208, 813
Vermeulen, R. C., Bernstein, R. A., Hough, D. H., & Readhead, A. C. S. 1993, ApJ, 417, 541
Vermeulen, R. C., & Cohen, M. H. 1994, ApJ, 430, 467
Wardle, J. F. C. 1995, private communication
Zensus, J. A., Bååth, L. B., Cohen, M. H., & Nicolson, G. D. 1988, Nature, 334, 410
Zensus, J. A., Cohen, M. H., & Unwin, S. C. 1995, ApJ, 443, 35
Zensus, J. A., Hough, D. H., & Porcas, R. W. 1987, Nature, 325, 36 (ZHP87)
Zensus, J. A., Krichbaum, T. P., & Lobanov, A. P. 1995, Proc. Natl. Acad. Sci., 92, 11348
Zensus, J. A., & Porcas, R. W. 1987, in Superluminal Radio Sources, ed. J. A. Zensus & T. J. Pearson (Cambridge: Cambridge Univ. Press), 126 (ZP87)